Journal of Radiotherapy in Practice

cambridge.org/jrp

Commissioning experience of the X-ray volume imaging system of an image-guided radiotherapy capable linear accelerator

Payal Raina and Susanta Kumar Sahoo

Department of Radiotherapy, Rajendra Institute of Medical Sciences, Ranchi, Jharkhand, India

Original Article

Cite this article: Raina P and Sahoo SK. (2021) Commissioning experience of the X-ray volume imaging system of an image-guided radiotherapy capable linear accelerator. *Journal of Radiotherapy in Practice* **20**: 108–113. doi: 10.1017/S1460396919001006

Received: 15 October 2019
Revised: 2 December 2019
Accepted: 5 December 2019
First published online: 13 January 2020

Key words:
contrast visibility; image-guided radiotherapy and quality assurance; spatial resolution; X-ray volumetric imaging system

Author for correspondence:
Payal Raina, Department of Radiotherapy, Rajendra Institute of Medical Sciences, E 2 Rashmi Enclave Arvind Marg, Bariatu, Bariyatu, Ranchi, Jharkhand 834009, India.
E-mail: payalraina2008@gmail.com

Abstract

Aim: An image-guided radiotherapy capable linear accelerator was installed at our hospital which is equipped with an X-ray volumetric imaging (XVI) system. The aim of this study was to describe the results of acceptance tests which were carried out on the XVI facility to verify the manufacturer's specification.

Materials and methods: The commissioning test had six elements: system safety, geometric accuracy, image quality, registration and correction accuracy, X-ray tube and generator performance, and quality assurance (QA) procedures.

Results: We had satisfactory results for all the tests. The system passed the safety testes, and the agreement of isocentres was found to be within the tolerance limit. Imaging quality was acceptable. Registration and correction accuracy was tasted with indigenously developed phantom and positioned accurately at isocentre. X-ray tube and generator test results showed that the tube was performing properly.

Findings: The described tests represent that the performance of the system is maintained at acceptable levels.

Introduction

Image-guided radiation therapy (IGRT) is the use of an imaging modality immediately prior to radiation therapy for the verification of patient and target location to improve the precision and accuracy of treatment delivery.[1] It depends on the accurate positioning of the patient during treatment to avoid detrimental effects of a geographic miss of tumour.[2] Historically, patient positioning is verified with megavoltage (MV) portal imaging, which has some limitations such as low subject contrast and use of two-dimensional (2D) projections of bony landmarks.[3] Nowadays, in-room kilovoltage (kV) cone beam computed tomography (CBCT)-based radiotherapy is becoming a widely accepted technique for target positioning due to its capability of providing a high-resolution planar radiograph and a high-contrast soft tissue volumetric image of the patient.[4] In our institution, Elekta Synergy (Elekta Limited, Crawley, UK) linear accelerator was installed in 2014 that uses a kV tube and a flat-panel amorphous silicon imager mounted opposite to each other across the drum of the accelerator head, known as the X-ray volumetric imaging (XVI) system. It acquires images under the control of the XVI software (Feldkamp–Davis–Kress algorithm) running on a dedicated XVI workstation. This XVI system has three different modes of kV image acquisition:[5] planar view—in this mode XVI acquires static 2D planar image; motion view—in this mode XVI acquires a sequence of 2D planar images over time, while the gantry moves; volume view—in this mode XVI acquires images while the gantry of the digital accelerator rotates. It has an option to choose different automatic registration modes, namely bone, grey value ($T + R$) and grey value (T) to match reference CT images with onboard CBCT images, where T and R represent 3D translation and rotation error. Bone mode of automatic registration uses a chamber matching algorithm. The chamber algorithm is not very sensitive to image noise, and XVI can calculate it quickly. The grey value ($T + R$) registration algorithm matches voxel grey scale intensity values in the specified region of interest (clip box). Grey value T is almost the same as grey value ($T + R$), but rotational error is not calculated for grey value T registration. At our institution, the linear accelerator upon which the CBCT system is mounted is in full clinical operation, following routine commissioning and calibration according to the reports of the American Association of Physicists in Medicine (AAPM) task groups 45 and 51.[6,7] The commissioning test had six elements: system safety, geometric accuracy, image quality, registration and correction accuracy, X-ray tube and generator performance and quality assurance (QA) procedures. In this study we compared the results of commissioning test results with manufacturer's specification. Additionally, we established a schedule of routine QA checks to ensure that the XVI system is accurate for patient positioning.

CAMBRIDGE UNIVERSITY PRESS

Material and Methods

The XVI system consists of a kV X-ray source arm and amorphous silicon panel detector. The generated X-ray is projected onto the plate of the kV detector for 2D and 3D imaging. The acquired beam is stored on the XVI workstation. For patient positing verification, the acquired image is superimposed on the corresponding planning CT and structure sets (anatomic contours), which are transferred to the XVI workstation from the treatment planning system via DICOM (Digital Imaging and Communications in Medicine). Table corrections are then given by the XVI software in *X, Y, Z* coordinates. To bring the patient into alignment with the reference geometry, the user needs to move the patient (couch) to correct the differences. A remote auto-setup tool is available. Precise table position can be adjusted after entering the treatment room, when necessary. To achieve accuracy in patient positioning, it is essential to carry out routine QA checks. The Elekta CBCT allows the width and length of the kV X-ray field to be selected. The width refers to the field of view (FOV), and the choices are small (S), medium (M) and large (L). The commissioning of the Elekta Synergy kV imaging system consists of five categories of tests: system mechanical safety, geometric accuracy (agreement of MV and kV beam isocentres), image quality (resolution and low contrast visibility), registration and correction accuracy. Tools required for the acceptance tests were Catphan CTP503, single ball-bearing phantom, 18 FG Leeds X-ray imaging phantom and a 1-mm copper filter plate.

System mechanical safety

This consists of a check of all system interlocks (door interlock, kV source arm interlock, terminate key) and of all the system touch guards (accelerator head, kV imaging panel arm, MV imaging panel arm). To test door interlock and kV source arm interlock, an attempt is made to deliver X-rays with either the door open or the kV source arm not fully extended. In addition, the door interlock is tested by opening the door while X-rays are being emitted. The terminate key is tested by pressing it while X-rays are being emitted.

Geometric accuracy

The alignment of the isocentres of kV imaging and MV treatment systems is crucial for accurate patient positioning, because the kV imaging system is used to position the patient with respect to the MV treatment system. This check is performed using a ball-bearing phantom supplied with the CBCT installation. The phantom consists of a steel ball (diameter 8 mm) located at the tip of a long plastic tube, which is connected to a base plate locked to the couch with a set of vernier adjustments that allow the position of the steel ball to be adjusted in 0·01 mm increments. For verification, the phantom was set at the isocentre and volume view image was acquired (Figure 1). After image registration, we manually moved the white ball in the three windows to align the virtual ball-bearing at the end of green tube in the coronal and sagittal image areas (Figure 2). We moved the ball bearing to the centre of the green tube in the transverse image area. After the positioning of ball bearing, we clicked the convert to correct button. The ball bearing was moved using the vernier scale to the quantities given by the correction window (Figure 2).

Image quality

Image quality achievable with the CBCT imaging system was tested for maximal achievable resolution and ability to display low-contrast objects. Catphan Phantom CTP503 (The Phantom Laboratory, Salem, NY) was used for image quality measurements. The phantom consists of various cylindrical sections (modules), each of which is designed for a specific test. For 3D uniformity testing, the top of the phantom was positioned in gantry direction as shown in Figure 3. S10 collimator cassette and F0 filter cassette into the kV source arm were used for imaging, and the kV imaging panel to the small FOV position was kept. Volume view image of Catphan was acquired as shown in Figure 4. The image was reconstructed. Uniformity module in the transverse image area was selected. In the transverse image area, five different locations

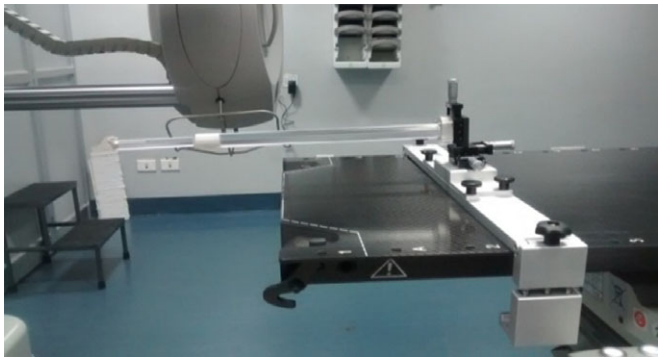

Figure 1. Positioning of ball-bearing phantom.

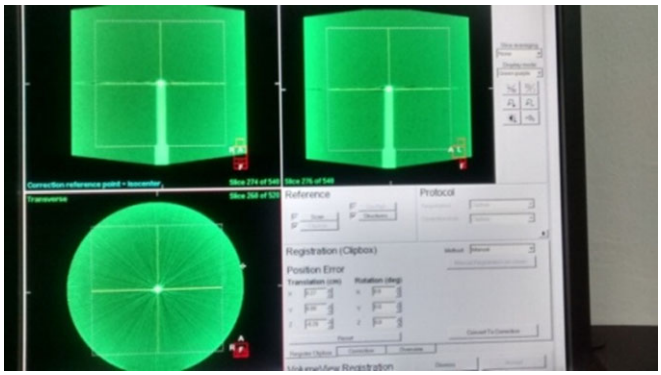

Figure 2. White ball positioning.

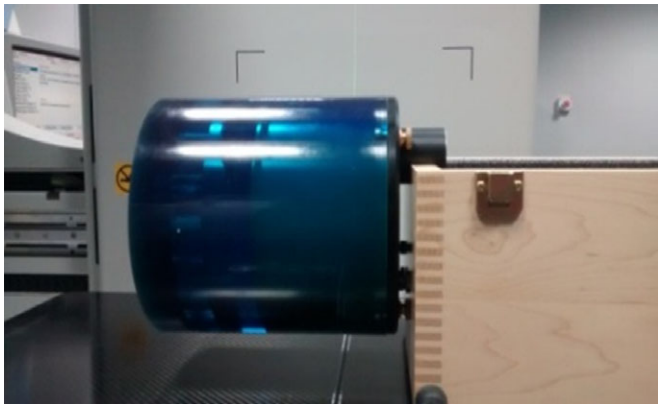

Figure 3. Catphan CTP 503 phantom in position.

https://doi.org/10.1017/S1460396919001006 Published online by Cambridge University Press

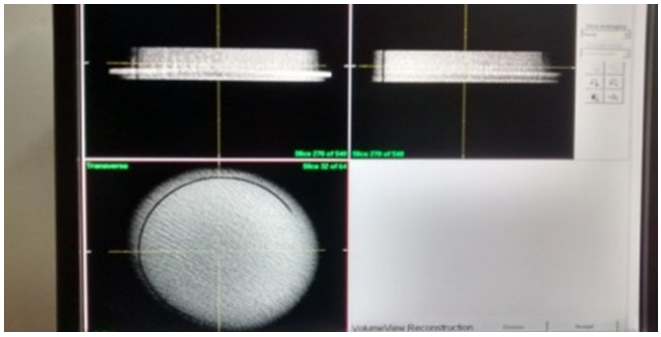

Figure 4. Uniformity module.

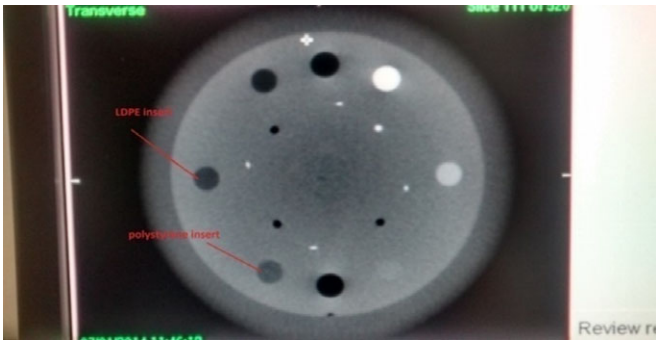

Figure 5. Contrast resolution module in Catphan CTP 503.

of the mean pixel values were measured. The maximum percentage difference of the highest mean pixel values was calculated by:

$$\frac{\text{Mean (high)} - \text{mean (low)}}{\text{Mean (high)}} \times 100\% \quad (1)$$

3D low-contrast visibility test between polystyrene and LDPE was performed. This measurement quantifies that the synergy XVI system can distinguish between fat and water.[8] Polystyrene is equivalent to fat and LDPT is equivalent to water. Volume view image of Catphan CTP503 was acquired as shown in Figure 5. In the transverse image area, contrast resolution module was selected. Low-contrast visibility was calculated by:

$$\text{Low contrast visibility \%} = \frac{\text{CT (polystyrene)} - \text{CT (LDPE)}}{10} * \frac{\{\text{SD (polystyrene)} + \text{SD (LDPE)}\}/2}{\text{Mean (polystyrene)} - \text{Mean (LDPE)}} \quad (2)$$

3D spatial resolution test measures the number of line pairs per centimetre resolved by the system. The test was done on Catphan CTP503 to the second alignment marker as shown in Figure 6. In 3D transverse vertical scale test, the distance between the two air inserts was measured and compared with specification as shown in Figure 7. In 3D transverse horizontal test, the distance between Delrin and LDPE inserts were measured and compared with specification (Figure 7). 2D low-contrast visibility test was checked with TOR 18FG Leeds phantom placed on a carbon fibre table top at the isocentre, with a 1-mm Cu plate positioned on top of the phantom as shown in Figure 8. Planar view

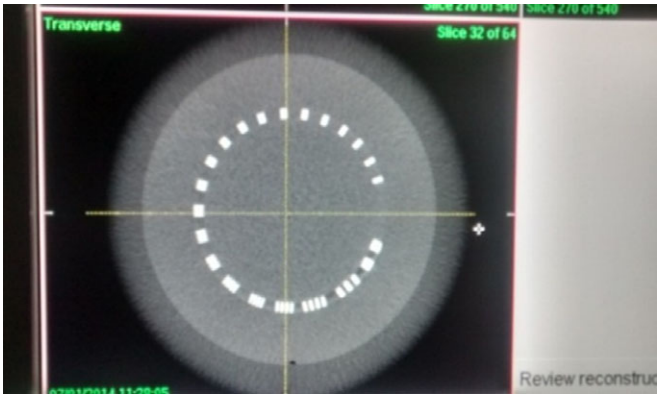

Figure 6. Spatial resolution transverse view.

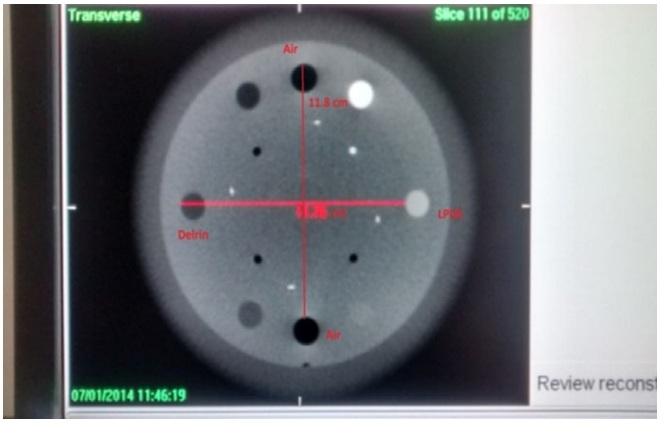

Figure 7. Distance between two inserts.

Figure 8. TOR 18FG phantom with 1-mm Cu plate position.

image was taken at a gantry angle of 270° with S20 collimator cassette and F0 filter cassette into the kV source arm. Brightness and contrast were adjusted such that both discs are clearly visible inside the squares. We counted the number of visible discs as shown in Figure 9. The greater the number of discs that are visible, the better the low-contrast visibility.[9] 2D spatial resolution test shows the minimum number of frequency groups that are visible as shown in Figure 10. A radiographic image of a phantom containing highly-absorbing (e.g. lead) thin lines at defined distances is used to visually assess the smallest distance at which the imaging system is capable of resolving the lines as separate entities.[10]

https://doi.org/10.1017/S1460396919001006 Published online by Cambridge University Press

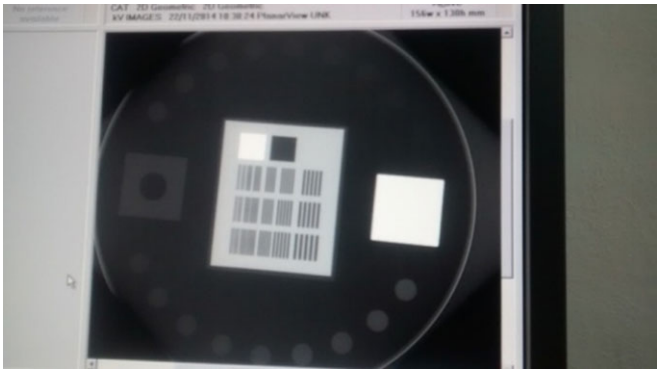

Figure 9. X-ray image of TOR 18FG phantom.

Figure 10. Visible frequency groups.

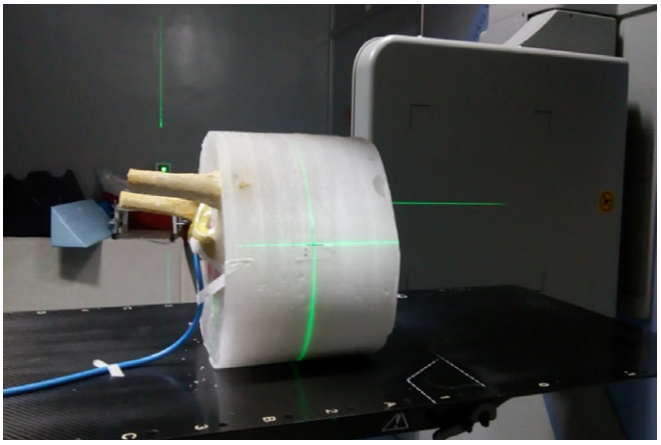

Figure 11. Pelvic phantom setup.

Registration and correction accuracy

The ability of the CBCT system to correctly register a localisation geometry with a reference geometry was tested using an indigenously developed pelvic phantom. The phantom was placed on the treatment couch by matching the fiducial marker with laser (Figure 11). After placing the phantom manually, we shifted the phantom along sagittal, longitudinal and lateral directions according to the shift given by the planning system to match the isocentre. Then we took the CBCT image. The acquired image was superimposed on the corresponding planning CT using grey value (*T*) automatic registration method, and we obtained table corrections in *X*, *Y* and *Z* directions (Figure 12). The table was corrected remotely. After correction, we manually shifted the table 10 mm 'right', then 'up' and finally 'in' to check the correction accuracy of the XVI system. Again, we took a CBCT image for verification.

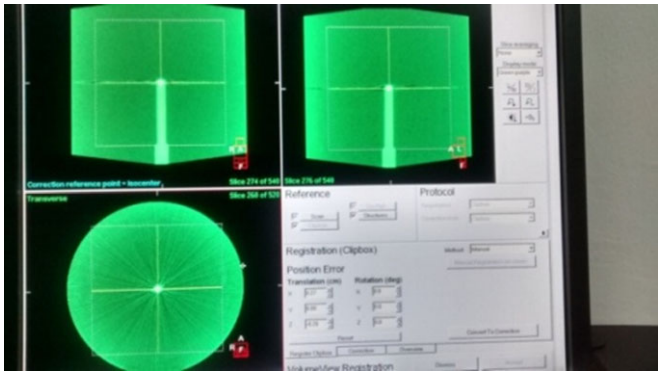

Figure 12. Transverse image of automatic registration of pelvic phantom.

X-ray tube and generator tests

As the CBCT imaging system consists of an X-ray generator, an X-ray tube and a digital imaging device, it is important to ensure that the generator and X-ray tube are performing properly so that imaging parameters can be confidently adjusted by the user. All the measurements were carried out by IBA Magic Max KV/Dose. The required tests are described below[11]:

(1) Accuracy of kVp

There is an optimal tube potential for each X-ray exposure. If peak energy of the output beam is not the same as the set kVp, important details of the image may be lost, resulting in retaking of image and hence more doses to the patient. If the percentage of kVp error lies within ±5%, the machine kVp value is acceptable.

(2) Accuracy of timer

Time is a very important parameter of an X-ray machine. A small variation in time might cause large dose variations, affecting both the patient and the image. More time gives more exposure to the patient, and less time of exposure gives poor-quality image. If the percentage of timer error lies within <10%, the machine time setting is acceptable.

(3) Total filtration

Determination of the half value layer (HVL) is an acceptable method for the specified quality of an X-ray beam. For a given kVp, a measurement of HVL gives information of total filtration (mm of Al) in the X-ray beam. Little filtration gives unnecessary radiation to the patient. The tolerance limit is 6 mm Al.

(4) Linearity of mA station

Tube current (mA) is equal to the number of electrons flowing from the cathode to the anode per unit time. Exposure of a beam for a given kVp and filtration is proportional to tube current. This

https://doi.org/10.1017/S1460396919001006 Published online by Cambridge University Press

test is carried out to check the linearity of radiation output with respect to change in tube current stations by keeping timer station constant at a particular kV station. The coefficient of linearity is calculated by:

$$\frac{X_{\max} - X_{\min}}{X_{\max} + X_{\min}}, \text{ where } X = \text{mGy/mAs} \quad (3)$$

(5) Linearity of timer

Exposure time is the duration of X-ray production. This test is carried out to check the linearity of radiation output with respect to change in timer stations. By keeping the kVp and mA constant, radiation output is measured at different timer stations, and coefficient of linearity was evaluated using formula (3).

(6) Output consistency

Keeping the mA and time fixed, radiation output is measured at various available kV stations to check the consistency of radiation output. The fixed average (X) of (mGy/mAs) is calculated. Consistency at each kV station was checked by evaluating the coefficient of variation by:

$$\frac{\sqrt{\frac{\sum_{i=1}^{n}(X_i - X)^2}{n-1}}}{X} \quad (4)$$

(7) Radiation leakage from the tube (mR)

Leakage from an X-ray machine is noted at 1 m distance from focal spot to front, back, right and left of the machine using the maximum field size. Tolerance limit is 100mR in 1 hour at 1 m.

Frequency of tests

Daily QA

Depending on the specifics of the system, the available interlocks should be tested on a rotational basis throughout the week. A phantom should be manually set up to an off-centre location. The phantom should be CBCT-imaged, aligned and moved to the isocentre.

Monthly QA

All available interlocks should be tested monthly. The isocentre of the kV CBCT system should be compared to the isocentre of the MV system. Daily QA of registration and correction accuracy should be repeated by the physicist performing monthly QA. The described image quality checks with Catphan should be performed. Preferably all tests should be done each month.

Annual QA

Safety tests and X-ray tube and generator tests should be performed annually, as described above.

Results

Each acceptance test was carried out and showed satisfactory results.

Table 1. Results of uniformity test

Measurement position	*X* coordinate (cm)	*Y* coordinate (cm)	*Z* coordinate (cm)	Mean pixel value
Position 1 centre	0·01	0·00	−0·01	768·84
Position 2	−4·51	0·00	0·03	761·49
Position 3	−0·01	0·00	−4·50	761·20
Position 4	4·50	0·00	−0·01	764·36

Table 2. Results of contrast insert

Insert	Mean pixel value	SD	Hounsfield unit (CT number)
Polystyrene	742·61	7·62	−35
LDPE	700·44	6·65	−100

System mechanical safety

The door interlock and beam termination at the control console worked correctly. A not-fully-extended kV source arm and an open door were shown in inhibit. All touch guards were found to work correctly.

Geometric accuracy

The maximal deviation of steel ball location from MV isocentre location was below the threshold of 0·25 mm.

Image quality

In 3D uniformity test, the maximum percentage difference of the highest mean pixel value was 0·99%, which meets the specification value of ≤1·5%. Pixel values at different positions measured by Catphan CTP503 are recorded in Table 1.

In 3D low-contrast visibility test, the percentage value of low-contrast visibility was 1·09%, which is within the specified value of ≤1·5%. Mean pixel value and standard deviation of polystyrene and LDPT for low-contrast visibility are recorded in Table 2.

In 3D spatial resolution test, the number of visible line pairs was 13 per centimetre, which meets the required specification of >10 line pairs per centimetre.

In 3D transverse vertical test, the measured distance between the two air inserts was 118·0 mm. The specified tolerance value is 117 ± 1·0 mm.

In 3D transverse horizontal scale test, the distance between Delrin and LDPE inserts was 118 mm. The actual distance was 117 mm. Tolerance is ±1·04 mm.

In 2D low-contrast visibility test, the number of visible discs was 15. The specification value was 12 minimum discs.

In 2D special resolution test, the number of visible frequency groups was 16, which meets the required specification of 10th group (1·4 line pairs/mm) as shown in Figure 10.

Registration and correction accuracy

Pelvic phantom was positioned accurately at the isocentre by taking a CBCT image.

https://doi.org/10.1017/S1460396919001006 Published online by Cambridge University Press

X-ray tube and generator tests

For the accuracy of KVp test, the applied KVp was 50 and measured KVp was 47·4 at 80 mA station within a tolerance limit of ±5 KV. For timer accuracy, the set time was 100 ms and observed time was 99 ms. Percentage error was 1%, which was within the tolerance of ±10%. The coefficient of linearity of the mA station was 0·0987 and of the timer was 0·012. Tolerance limit for the coefficient of linearity was <0·1. The result was within the tolerance limit. Total filtration (mm of Al) of the X-ray tube was 8·3 mm of Al, which is within the tolerance limit of 6 mm Al. The coefficient of variation for output consistency was $6{\cdot}6 \times 10^{-4}$ for 70 kV. Tolerance value was <0·05 for output consistency. This shows that the result was within the limit. Radiation leakage from the tube was 37·5 mR in 1 hour at 1 m, which is within the tolerance limit of 100 mR in 1 hour at 1 m.

Discussion

Because patient positioning is directly based on data from the XVI system, their performance has a major effect on treatment outcome. Therefore, the accuracy and reliability of CBCT systems need to be tested. The set of tests presented here was performed before using XVI for clinical purposes. The described tests represented clinical reality and ensured that the performance of the system was maintained at acceptable levels. The results also matched with other reports. AL-Jasim Ali Kareem et al.[12] performed quality control tests to evaluate the performance of the equipment. kV accuracy test, kV reproducibility, time accuracy, X-ray beam collimation, HVL/filtration and leakage radiation were performed, which complied with the requirements of the standards and manufacturer's specifications, similar to our study. Joerg Lehmann[13] suggested the frequency of QA procedures. An anthropomorphic skull phantom and Rando phantom were used for registration and correction accuracy. In our study, we used an indigenous heterogeneous pelvic phantom. All the results matched with their study. According to the Radiation Safety Training Module: Diagnostic Radiology Quality Assurance in Diagnostic Radiology of the Atomic Energy Regulatory Board (AERB), India,[14] our results were within the tolerance levels.

Conclusions

Image-guided therapy and kV cone beam computed tomography are powerful tools in a modern radiation oncology facility. For accurate patient treatment, appropriate functioning of all systems is most important. With the XVI system, the patient can be objectively and precisely positioned for treatment. Our acceptance test results showed that the XVI system can be clinically used with routine QA programme.

Acknowledgements. We would like to thank the team at the radiotherapy department for their cooperation in taking measurements.

Financial support. None.

Conflicts of interest. There are no conflicts of interest.

References

1. Van Herk M. Different styles of image-guided radiotherapy. Semin Radiat Oncol 2007; 17: 258–267.
2. Verellen D, De Ridder M, Linthout N, Tournel K, Soete G, Storme G. Innovations and advances in radiation technology. Nat Rev Cancer 2007; 7: 949–960.
3. Verellen D, De Ridder M, Storme G. A (short) history of image-guided radiation therapy. Radiother Oncol 2008; 86: 4–13.
4. Li T, Schreibmann E, Yang Y, Xing L. Motion correction for improved target localization with on board cone-beam computed tomography. Phys Med Biol 2006; 51 (2): 253–267.
5. Letourneau D, Wong JW, Oldham M et al. Cone-beam-CT guided radiation therapy: technical implementation. Radiotherapy Oncol 2005; 75: 279–286.
6. Almond PR, Biggs PJ, Coursey BM et al. AAPM's TG-51 protocol for clinical reference dosimetry of highenergy photon and electron beams. Med Phys 1999; 26 (9): 1847–1870.
7. Nath R, Biggs PJ, Bova FJ et al. AAPM code of practice for radiotherapy accelerators: report of AAPM Radiation Therapy Task Group No. 45. Med Phys 1994; 21 (7): 1093–1121.
8. Letourneau D, Wong JW, Oldham M et al. Cone-beam-CT guided radiation therapy: technical implementation. Radiother Oncol 2005; 75 (3): 279–286.
9. Oldham M, Letourneau D, Watt L et al. Cone-beam-CT guided radiation therapy: a model for on-line application. Radiother Oncol 2005; 75 (3): 271–278.
10. Groh BA, Siewerdsen JH, Drake DG, Wong JW, Jaffray DA. A performance comparison of flat-panel imger-based MV and KV cone-beam CT. Med Phys 2002; 29 (6): 967–975.
11. Lehmann J, Perks J, Semon S, Harse R, Purdy JA. Initial experience with CBCT and IGRT. Int J Radiation Oncol Biol Phys 2006; 66: 620–621.
12. AL-Jasim AK, Hulugalle SNCWMPSK, Al-Hamadani HK. A Quality Control Test for General X-Ray Machine. WSN 2017; 90: 11–30.
13. Lehmann J, Perks J, Semon S, Harse R, Purdy JA. Commissioning experience with cone-beam computed tomography for image-guided radiation therapy. J Appl Clin Med Phys 2007; 3 (8): 21–36.
14. Atomic Energy Regulatory Board (AERB), SAFETY CODE NO.AERB/RF-MED/SC-3 (Rev. 2). Radiation safety in Manufacture, supply and use of medical diagnostic X-ray Equipment, 2016.

https://doi.org/10.1017/S1460396919001006 Published online by Cambridge University Press